INTERACTION BETWEEN γ- PHASE PRECIPITATES AND MARTENSITE IN CU-ZN-AL ALLOYS

J. Pons and E. Cesari

Departament de Física, Universitat de les Illes Balears, Ctra. de Valldemossa, km. 7.5, E-07071 Palma de Mallorca, Spain, e:mail: dfsjpm0@ps.uib.es

1. Introduction

One way of strengthening the Cu-based shape memory alloys (and approaching to the performances of Ni-Ti alloys) is through the introduction of γ-phase precipitates in the β phase matrix. The thermal treatments suitable to generate distributions of precipitates of different sizes and densities are well known [1-4]. However, the presence of precipitates produces changes in the martensitic transformation temperatures and the hysteresis accompanying the forward and reverse transformations [1, 5-7]. A systematic study on this subject has been carried out in the recent last years, specially in Cu-Zn-Al single crystals with compositions in the vicinity of 16%at Al -15%at Zn, having an electron-to-atom ratio of 1.48 [5-13]. The present paper will show the most relevant results obtained.

2. Generation of Precipitates

The first studies on γ precipitation in single crystalline Cu-Zn-Al shape memory alloys with e/a = 1.48 were performed by Chandrasekaran, Rapacioli and Lovey [1-4]. Distributions of γ-type precipitates are obtained in alloys with more than 10 at% Al by means of a non-equilibrium way consisting in quenching from temperatures in the range 670 K - 920 K to a temperature below 350 K but still in the β condition. The last requirement is essential, *i.e.* when quenching directly to the martensitic phase, the precipitates are not observed. Along the present paper, we will refer to this kind of quenching as treatment TTB (typically, quenching from 770 K). The precipitates obtained in this way are coherent with the β phase (Fig. 1) and range in size from 10 to 100 nm, depending on the quenching temperature.

The precipitates obtained on quenching can be grown by subsequent upquenching or flash heating to intermediate temperatures (typically 670 K). Examples of the distributions obtained after short and long flash heating times are shown in Fig. 2. During its growth, the precipitates lose the coherency with the β matrix, becoming semicoherent. This happens when they reach sizes of about 100 nm. The semicoherent precipitates develop a network of interface (misfit) dislocations on their faces, with <100> Burgers vectors in the {100} faces and also 1/2<111> and <100> Burgers vectors in the {110}faces [7, 14, 15] (Fig. 3).

Precipitates of γ phase can also be nucleated and grown by the flash heating treatment even in the absence of the small precipitates mentioned above, *i.e.* in fully betatized specimens, quenched from temperatures in the region of β stability (typically 1120 K), which will be called treatment TTA. In such a case, the precipitate distributions obtained are generally less dense than those obtained with the same flash heating applied after a TTB treatment. Thus, a wide range of precipitate distributions (with different densities and precipitate sizes) can be generated in a controlable way

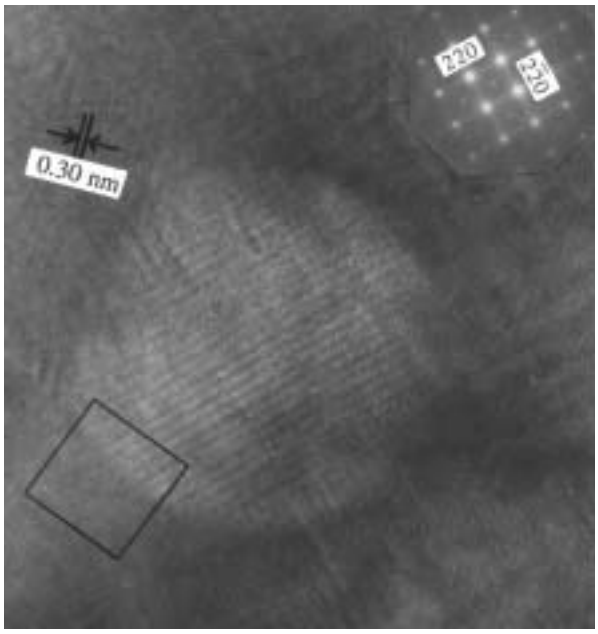

Figure 1. (a) HREM image of a precipitate coherent with the β matrix.

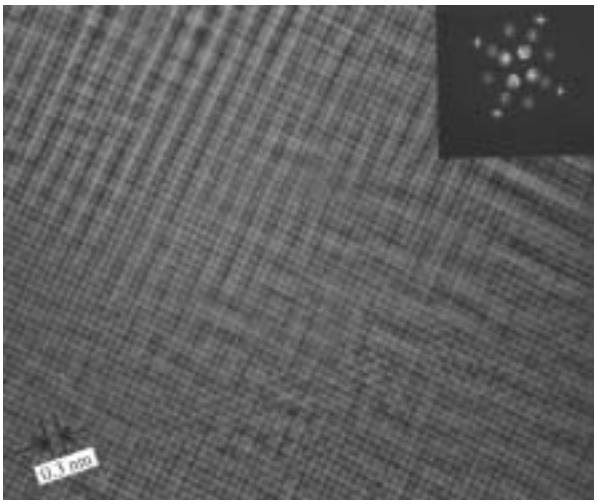

Figure 1. (b) Enlarged and Bragg-filtered image of the framed region of (a), showing the perfect continuity of atomic planes in the precipitate and the matrix.

by the combination of the first quenching (TTA or TTB) and the subsequent flash heating.

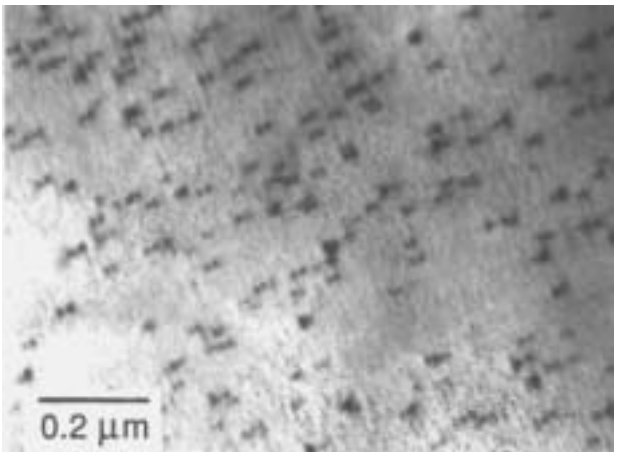

a)

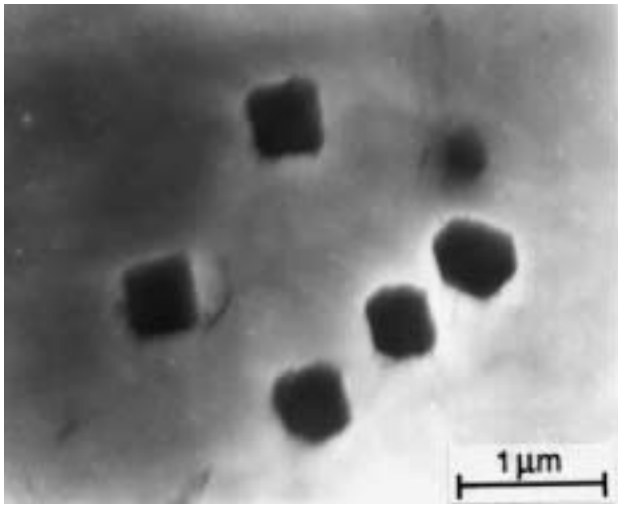

b)

Figure 2. Distributions of precipitates obtained after a treatment TTB and flash heating at 670 K for 20s (a) and 60 s (b)

3. Influence of Precipitates on the Martensitic Transformation

3.1 Macroscopic results. Effects on the transformation temperatures

The effects of precipitates can be assessed by comparing with precipitate free samples of the same alloys, submitted to a reference thermal treatment (air cooling from the β stability region, typically 1120 K). The main trends of the observed effects are as follows [5-7]: when the precipitates are small and coherent with the β matrix, the transformation temperatures are lowered and the hysteresis slightly widened compared to the reference values. For instance, a drop of Ms (and Af) by about 15 K is observed in samples submitted to TTB and 20 s flash heating at 670 K. When the precipitate size grow, the Ms and Mf values continue to fall, but As and Af stop their falling and start to increase (even at higher values than the reference ones), giving rise

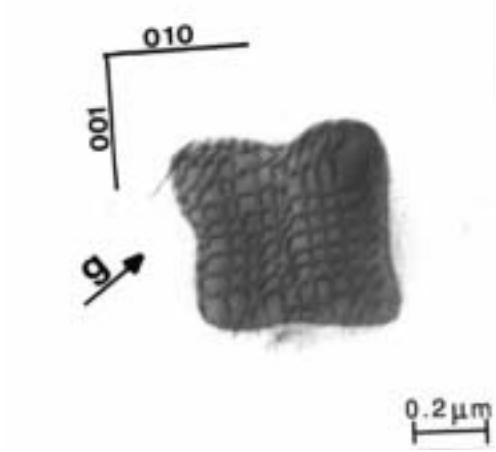

a)

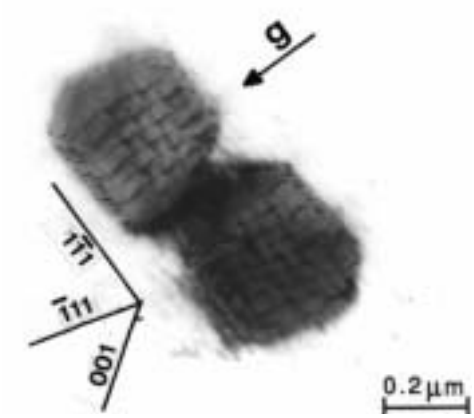

b)

Figure 3. (a) Misfit dislocations in the {100} face observed under two beam condition with **g** = [01$\bar{1}$] (b) Misfit dislocations in the {110} face, **g** = [1$\bar{1}$2]

to a considerable increase of transformation hysteresis. For instance, in samples with TTB and 60 s at 670 K, the hysteresis (Af-Ms) is about 60 K, while the reference value is about 5 K. When the semicoherent precipitates grow further, the direct transformation temperatures also revert their previous behaviour and start to increase. For very large precipitate sizes (of the order of 1 μm), as after a flash heating of 180 s at 670 K, all transformation temperatures except Mf are shifted to values higher than the reference ones. The samples submitted to TTA treatment and flash heating exhibit a similar behaviour.

Not only the size of precipitates is important, but also the density of the precipitate distributions. In samples treated in a special way (15 min. homogenization at 920 K and cooling to room temperature at a controled rate of 50 K/s, treatment called TTC) and subsequently flash heated at 670 K for different times (up to 100 s), distributions of big precipitates (about 1 μm size) are obtained already for the shortest flash heating times, but with a much lower density compared to those with similar precipitate sizes obtained after a TTB or TTA and flash heating treatment. In the case of TTC as the first thermal treatment, all the transformation temperatures are higher than the reference ones,

but the hysteresis is only slightly raised (it is always less than 10 K for flash heating times up to 100 s) [6,7].

3.2 Microscopic observations. Interaction between γ precipitates and martensite

As commented above, the γ precipitates are rather well accommodated with the parent β phase: they are either fully coherent or, at most, semicoherent, depending on the precipitate size. This is due to the cubic-cubic orientation relationship between the β and γ phases and the small misfit between the two cubic lattice parameters ($\varepsilon \cong 7.5\ 10^{-3}$ [14]). Nevertheless, when the matrix surrounding one precipitate is transformed to a single variant of martensite, the hole left in the β matrix occupied by the precipitate is quite severely deformed due to the intrinsic deformation accompanying the transformation [11], but the precipitate itself maintains its shape (the γ phase does not transform martensitically). TEM observations show that the martensite plates indeed absorb completely the small precipitates (with sizes up to 300 nm) found during its growth. Thus, strong stresses arise around the precipitates due to the transformation shape change. The difficult accommodation between martensite and precipitates requires an extra elastic energy, which is responsible for the observed shift of the transformation to lower temperatures. At this stage, the effects on the transformation temperatures increase with the precipitate size, as the accommodation energy also increases. In fact, the accommodation is not completely elastic, but plastic deformation of the surrounding martensite occurs, which is evidenced by the HREM observation of dislocations in martensite around the precipitates [10]. The same observations show the formation of martensite nanoplates at the interface between the precipitate and the main martensite plate. The nanoplates are self-accommodating with the main plate (Fig. 4). The dislocations form in martensite, but they remain in the β phase after the reverse transformation takes place, due to the diffusionless character of the martensitic transformation. When the thermal transformation is repeated many times, dislocation arrays around the precipitates and far from them can be observed by conventional TEM (Fig. 5) [8]. In the case of stress-induced transformations (single martensite variant), dislocations loops encircling the precipitates can be observed by the weak-beam dark field technique after a transformation-retransformation cycle (Fig 6). These loops are responsible for the changes observed in the σ–ε curves [12,13] as well as for an easier induction of the two-way shape memory effect in the samples containing coherent precipitates [9].

When the precipitates attain a critical size of about 300 nm, they can not be completely absorbed by a single martensite plate, because the deformation that it would be necessary to accommodate around the precipitate becomes too large. Instead, a complex array of small martensite plates form in between the precipitates (Fig 7). This change of martensite microstructure reduces the elastic energy required for the martensite-precipitate accommodation. The elastic energy reduction, together with the chemical effects of precipitates (the matrix around the precipitates is depleted in Al), account for the observed increase of transformation temperatures. The increase of hysteresis is also related with the change of martensite microstructure. In this stage, the effects are not directly dependent on the precipitate size, but mainly on the density of the precipitate distribution, i.e. on the separation between precipitates, which limitates the size of the martensite plates. This is evident when comparing the results from the TTB or TTA with those of TTC treatments. Again, the martensite/precipitates accommodation is not completely elastic: big arrays of dislocations can be observed near the precipitates after repeating many times the thermal transformation (Fig. 8). Once these dislocations are formed, they improve the martensite accommodation for the subsequent cycles, which is re-

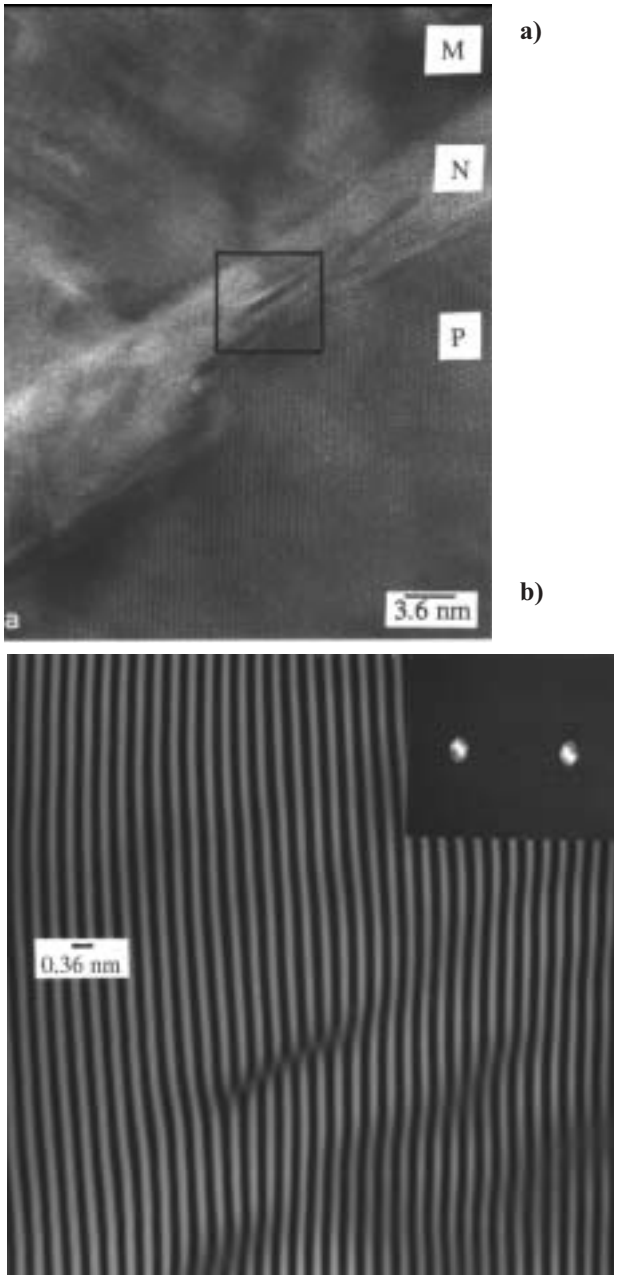

Figure 4. (a) HREM image of the interface between a precipitate (P) and martensite (M). A nanometric martensite plate (N) of a variant self-accommodating with M is formed at the precipitate interface. (b) Enlarged and Bragg-filtered image of the framed region of (a). Note the presence of a dislocation in the nanoplate (N).

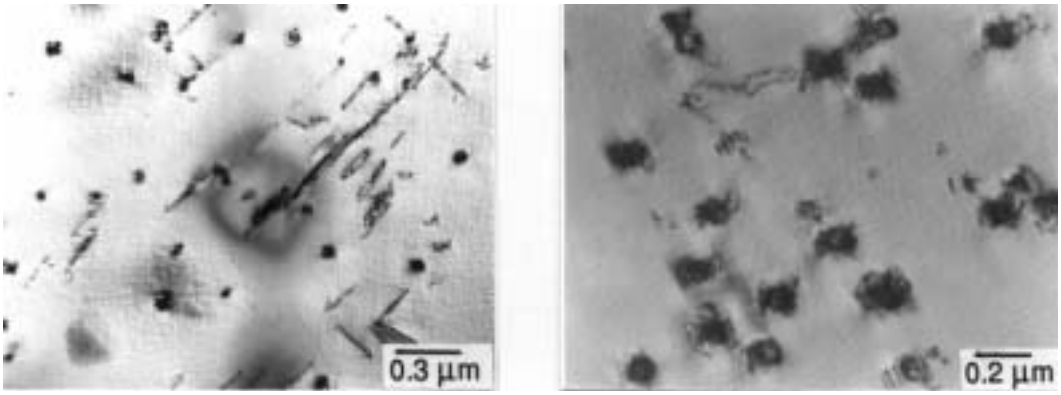

a) b)

Figure 5. Dislocations formed around the precipitates in samples with 10 thermal cycles. (a) sample with TTB; (b) sample with TTB plus flash heating of 10 s at 670 K.

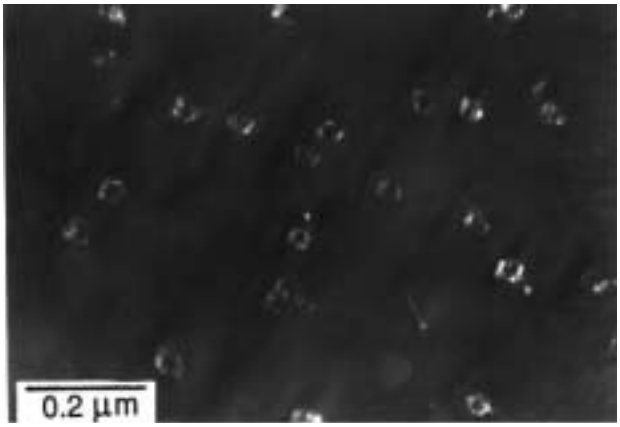

Figure 6. Weak-beam dark field image of the dislocation loops formed around the precipitates in a sample with 605 pseudoelastic cycles.

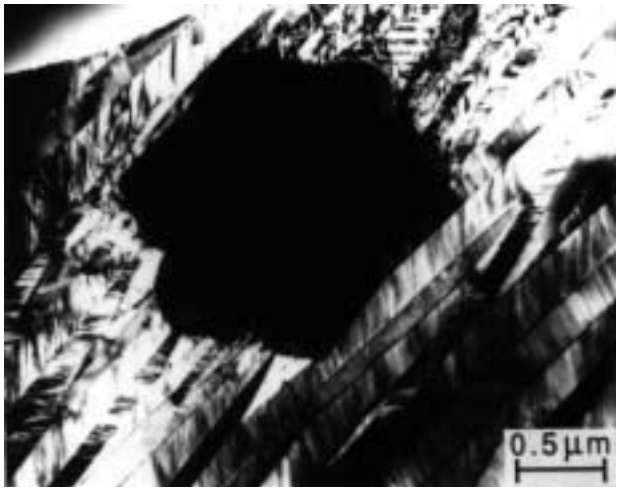

a)

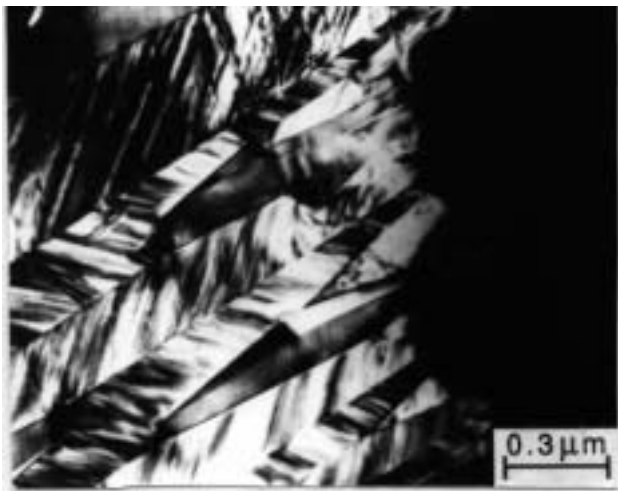

b)

Figure 7. (a) TEM image of the small martensite plates formed around a big precipitate, (b) detail of (a)

flected in a progressive shift of the direct transformation temperatures towards the reference values during thermal cycling [8].

4. Conclusions

A variety of distributions of γ-phase precipitates in Cu-Zn-Al single crystals with e/a=1.48, with different size, shape, distribution density and nature (coherent or semi-coherent) can be obtained by some suitable thermal treatments. They bring about very different effects on the martensitic transformation temperatures, which are mainly related with the difficulties in the martensite/precipitate accommodation due to the intrinsic deformation of the martensitic transformation. The microstructural observations (mainly TEM and HREM) allow for a better understanding of the observed effects.

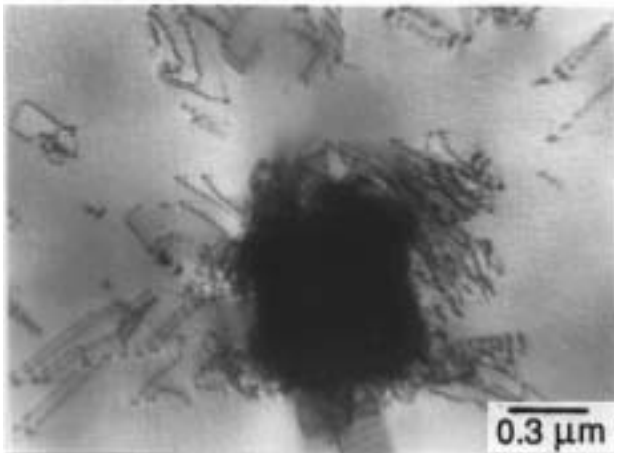

Figure 8. Dislocations formed around a precipitate in a sample submitted to TTB + 60s at 670K and 10 thermal cycles

Acknowledgements

Partial finantial support from the DGES (Spain), project PB95-0340, is gratefully acnowledged.

References

1. R. Rapacioli, M. Chandrasekaran; *Proc. ICOMAT'79*, MIT, Cambridge, MA (1979), p. 596.
2. R. Rapacioli, M. Chandrasekaran, F.C. Lovey; *Proc. Int. Conf. Solid-Solid Phase Transf.* , Met. Soc. AIME, Warrendale, PA, (1982), p. 739.
3. F.C. Lovey, R. Rapacioli, M. Chandrasekaran; *Phys. stat. solidi (a),* **68** (1981) K105.
4. F.C. Lovey, G. Van Tendeloo, J. Van Landuyt, M. Chandrasekaran, S. Amelinckx; *Acta Metall.*, **32** (1984) 879.
5. C. Auguet, E. Cesari, R. Rapacioli, Ll. Mańosa; *Scripta Metall.*, **23** (1989) 579.
6. J. Pons, E. Cesari; *Thermoch. Acta*, **145** (1989) 237.
7. J. Pons, *Ph D. Thesis*, Universitat de les Illes Balears (Spain), 1992.
8. J. Pons, E. Cesari; *Acta Metall. Mater*., **41** (1993) 2547.
9. J. Pons, M. Sade, F.C. Lovey, E. Cesari; *Mater. Trans JIM*, **34** (1993) 888.
10. J. Pons, R. Portier; *Acta Mater*., **45** (1997) 2109.
11. F.C. Lovey, V. Torra, A. Isalgué, D. Roqueta, M. Sade; *Acta Metall. Mater*., **42** (1994) 453.
12. D. Roqueta, F.C. Lovey, M. Sade; *Scripta Mater.*, **34** (1996) 1747.
13. D. Roqueta, *Ph. D. Thesis*, Instituto Balseiro - Centro Atómico Bariloche (Argentina), 1997.
14. F.C. Lovey, E. Cesari; *Mat. Sci. Eng*., **A129** (1990) 127.
15. M. Chandrasekaran, J. Pons, E. Cesari; *Proc. 10th European Conf. on Electron Microscopy*, A. López-Galindo and M.I. Rodríguez-García, (eds.), vol. IIA, 1992, p. 241.